UDK 669.058.4
Original scientific article/Izvirni znanstveni članek

ISSN 1580-2949
MTAEC9, 57(1)27(2023)

PREPARATION AND HARDNESS OF A FUNCTIONALLY GRADED Ni-Al COATING

PRIPRAVA IN TRDOTA PREVLEKE NA OSNOVI Ni-Al

Ningning Li, Lei Xu, Liang Huang, Yuping Tong, Zhengquan Jiang*, Keliang Li

North China University of Water Resources and Electric Power, School of Materials Science and Engineering, Zhengzhou

Prejem rokopisa – received: 2022-10-10; sprejem za objavo – accepted for publication: 2022-12-05

doi:10.17222/mit.2022.650

A functionally graded Ni-Al coating can improve the hardness of low-carbon steel, which can then adapt to various conditions due to a high hardness. The primary purpose of this research was the preparation of a Ni-Al coating by adopting a two-step method including nickel plating and pack aluminizing. The coating phase and morphology were characterized with XRD, SEM and EDS. Subsequently, the hardness of the Ni-Al coating was measured using a nanoindentation test. The results show that different aluminum contents in the coating surface lead to different coating phases, mainly Ni_2Al_3. The change in the coating phases conformed to the Ni-Al binary phase diagram. The Ni-Al coating showed a continuous gradient structure and composition. In addition, the coating also showed continuous gradient variation, relating to the hardness.

Keywords: Ni_2Al_3 coating, nanoindentation, hardness, gradient

Funkcionalnim prevlekam Ni-Al se lahko po preseku spreminja sestava in temu primerno tudi fizikalne lastnosti. Osnovni namen raziskave, opisane v članku, je bila priprava prevlek Ni-Al z dvostopenjsko metodo elektro platiranja niklja in paketnega aluminiziranja (angl.: pack aluminizing). Faze prevlek in njihovo morfologija so bile določene z rentgensko difrakcijo (XRD), vrstično elektronsko mikroskopijo (SEM) in elektronsko disperzijsko spektroskopijo (EDS). Sledile so še meritve nanotrdote izdelanih prevlek Ni-Al s postopkom nanovtiskovanja oziroma kontroliranim vtiskovanjem nanoprizme. Rezultati analiz so pokazali, da različna vsebnost Al na površini prevleke vodi do nastanka različnih faz, predvsem faze Ni_2Al_3. Spremembe fazne sestave v prevleki se ujemajo z binarnim faznim diagramom Ni-Al. Izdelane prevleke na osnovi Ni-Al kažejo neprekinjen gradient strukture in sestavo. Istočasno se v skladu s tem zvezno spreminjajo tudi njihove fizikalno-kemijske lastnosti, kar se predvsem odraža na izmerjeni nanotrdoti.

Ključne besede: prevleka na osnovi Ni_2Al_3, nano vtiskovanje, trdota, gradient

1 INTRODUCTION

Functionally graded materials (FGMs) refer to a class of non-homogeneous composite materials with continuous and quasi-continuous changes in the structure and elements, exhibiting the performance and composition change in the gradient. Their microstructures, physical, chemical and biological properties show continuous changes in a single phase, or a combination of phases, to achieve a particular function. FGMs are one of the crucial topics relating to the current structural and functional materials.[1] A functionally graded coating is classified according to the changes in the composition, relating to the surface technology area, and its potential applications are primarily found in high-temperature, wear, corrosion and other areas.[2,3]

The preparation methods for a functionally graded coating include vapor deposition,[4] plasma spraying,[5] laser cladding[6], etc. A vapor-deposition coating is very thin. Plasma spraying is subject to power restriction where the processes are complex and difficult to control, and the coating bonding strength is poor. The high energy of the laser-cladding method may damage the properties of the matrix.

In recent years, several intermetallic compound coatings have been researched due to their high melting points, low densities and excellent corrosion resistance at high temperatures. Ni-Al intermetallic compound coatings have been applied to high-temperature alloy surfaces because they can easily form a dense alumina layer at high temperatures.[7,8] Pack aluminizing is the favored method that can be used for preparing nickel-aluminum coatings on Ni-based alloys. To apply a nickel-aluminum coating onto another metal surface, a two-step process including nickel plating and powder aluminizing has been invented.[9–11] In addition to exhibiting the advantages of good quality, simple operation, minor technical difficulties and low investment in the equipment, this method also reduces the influence of the chemical composition of the substrate on forming an aluminized coating so that a low aluminized temperature can be used. According to recent research, the low temperature can also protect the substrate properties.

In this study, we investigated the synthesis of a functionally graded Ni-Al coating on a substrate by adopting a two-step method including plating nickel and pack aluminizing. The coating composition and morphology were characterized with XRD, SEM and EDS. The hardness was tested with nanoindentation.

*Corresponding author's e-mail:
jiangzhq@ncwu.edu.cn (Zhengquan Jiang)

2 EXPERIMENTAL PART

2.1 Materials

To carry out the research conveniently, the ordinary Q235 steel was selected as the substrate, with dimensions of (10 × 10 × 2) mm; its nominal chemical composition is shown in **Table 1**. Before plating, the substrate was mechanically polished with metallographic papers, polished and ultrasonically cleaned with acetone for 5 min, then washed with distilled water and activated in 5 *w*/% HCl for 20 s; finally, it was washed with distilled water again and quickly immersed into a bath.

The basic Watts nickel composition and plating conditions are shown in **Table 2**. The chemicals used are of analytical grade and dissolved in distilled water. The solution pH value was adjusted to 4.0 for H_2SO_4 (20 *w*/%). The electroplating power supply was a DC power supply. For maintaining the solution homogeneity, mechanical stirring by a magnetic stirrer located at the container bottom was used. Four nickel-plated samples were prepared. The samples were washed with distilled water and ethanol repeatedly, being removed from the cell.

The pack mixture is composed of the Al powder, $AlCl_3$ and Al_2O_3 powder reminder as the filler. Alumina power needs to be used after high-temperature calcinations. $AlCl_3$ was used without any processing after being removed from the reagent bottle. Previous studies showed that the content of aluminum powder has the greatest impact on the coatings phases.[12] In order to explore the Al-powder role in the formation of a Ni-Al functionally graded coating, a series of samples was manufactured, and the contents of the Al power were (8, 15, 50 and 70) *w*/%. For the convenience of discussion, they were defined as Sample 1, Sample 2, Sample 3 and Sample 4, respectively. The activating $AlCl_3$ content was 5 *w*/%, and the Al_2O_3 reminder was the inert filler. The pack aluminizing process is described as follows: the substrate was embedded in a packed mixture in an alumina crucible and then positioned in a vacuum tube furnace with argon. The furnace was heated at a rate of 10 °C/min and the dwell time was 20 h at a temperature of 650 °C. Eventually, the samples were removed after having been cooled down to room temperature, and alcohol was used to remove the adhered particles.

2.2 Hardness test

The hardness of the coatings was measured with a nanoindentation test; the CSM instrument, which came from Switzerland, was equipped with a diamond Berkovich indenter. The maximum applied load was 50 mN, the holding time was 10 s, while the loading and unloading rates were 100 mN/min.

2.3 Surface characterization

The phase composition of the surfaces of the coatings was identified using X-ray diffraction (XRD) with a CuK_a radiation (D/Max-RA, Rigaku, Japan). The chemical compositions and microstructures at the cross-sections of the coatings were tested with SEM and energy-dispersive spectroscopy (EDS) (S-3400II, Hitachi, Japan).

3 RESULTS AND DISCUSSION

3.1 Coating phases of pack aluminizing with different Al amounts

XRD results are shown in **Figure 1,** namely, the phase results for different coatings, which show that the four samples have different phases. Sample 1 has a single Ni_2Al_3 phase, while Samples 2, 3 and 4 are composed of Ni_2Al_3 and $NiAl_3$ of different ratios. The formation of varying phases will be discussed in combination with other data in Section 3.5.

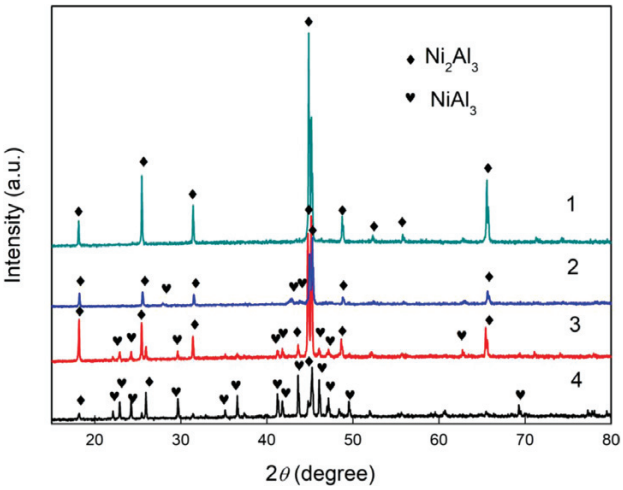

Figure 1: XRD patterns for different coating surfaces

Table 1: Nominal chemical composition of Q235 low-carbon steel (*w*/%)

Composition	C	Mn	Si	S	P	Fe
Content	0.140–0.220	0.300–0.650	0.300	≤ 0.050	0.045	Bal.

Table 2: Chemical composition of the Watts Ni bath and the electro-deposition conditions

Composition	$NiSO_4{\cdot}6H_2O$	$NiCl_2{\cdot}6H_2O$	H_3BO_3	*T*	pH	Agitation
Parameter	240 g/L	20 g/L	30 g/L	45–60 °C	4.0	Magnetic stirrer

3.2 Chemical morphologies and compositions of aluminized coating surfaces

Figure 2 represents different coating-surface morphologies, while **Table 3** shows the components of different coating surfaces.

As can be seen, the morphologies of the coatings are different. **Figure 2a** represents the single Ni_2Al_3 phase, fabricated using an 8 *w*/% Al-power amount, and its surface as a whole is relatively flat. The EDS result shows that the coating components are 58.57 *x*/% Al, 40.99 *x*/% Ni and 0.44 *x*/% Fe (atomic %). The XRD data analysis consists of a phase diagram of Ni-Al.[13] **Figure 2b** shows the coating fabricated with 15 *w*/% Al powder. Exhibiting a sharp contrast, its appearance is relatively rough. More Fe is detected with the EDS results. The Al content is 64.78 *x*/%, and the phases are $NiAl_3$ and Ni_2Al_3, combined, in the two-phase region, in the Ni-Al diagram. This result is consistent with XRD, and when the peak intensity of Ni_2Al_3 is much stronger than that of $NiAl_3$, it is clear that the Ni_2Al_3 phase prevails. **Figures 2c** and **2d** show the Ni-Al layer fabricated with 50 *w*/% and 70 *w*/% Al powder, and the apparent difference is the Fe element that is not detected on the two coating surfaces. The Al contents are 73.93 *x*/% and 74.96 *x*/%, which means that the $NiAl_3$ phase prevails. This is also confirmed with the XRD result.

$NiAl_3$ and Ni_2Al_3 are the two typical phases that are easy to form; their melting points are 854 °C and 855–1133 °C. By comparison, $NiAl_3$ is not expected to appear in the coating. However, the three layers are prepared with pack Al-powder amounts of 15 *w*/%, 50 *w*/% and 70 *w*/%, and they all contain a $NiAl_3$ phase. Therefore, in the following discussion, this paper mainly focuses on the Ni_2Al_3 coating to explore its microstructure and properties.

3.3 Cross-sectional microstructure and composition of the Ni_2Al_3 coating

Figure 3 shows SEM and EDS results for the cross-sectional microstructure and composition of the Ni_2Al_3

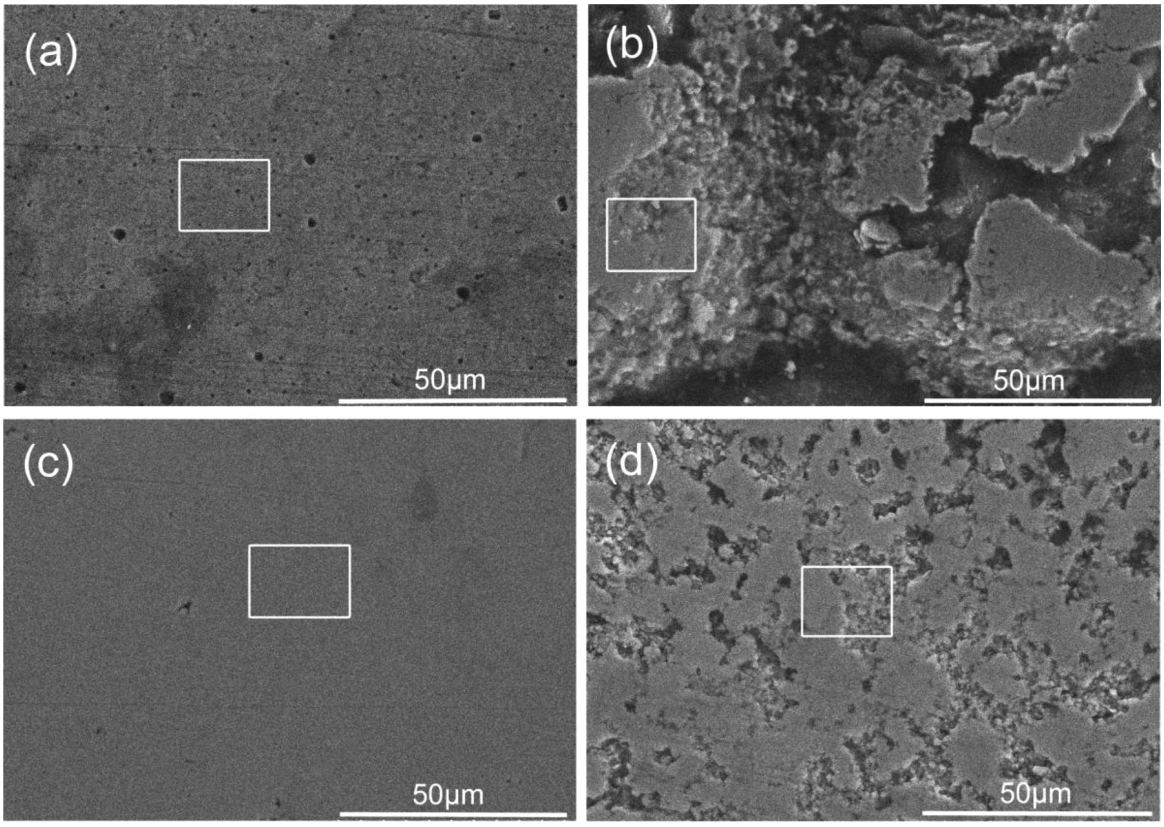

Figure 2: Surface morphologies of different coatings fabricated using different pack Al-power amounts: a) 8 *w*/%, b) 15 *w*/%, c) 50 *w*/%, d) 70 *w*/%

Table 3: Components of different coatings (*x*/%)

Material components	Sample 1	Sample 2	Sample 3	Sample 4
Al	58.57	64.78	73.93	74.96
Ni	40.99	23.28	26.07	25.04
Fe	0.44	11.94	0.00	0.00

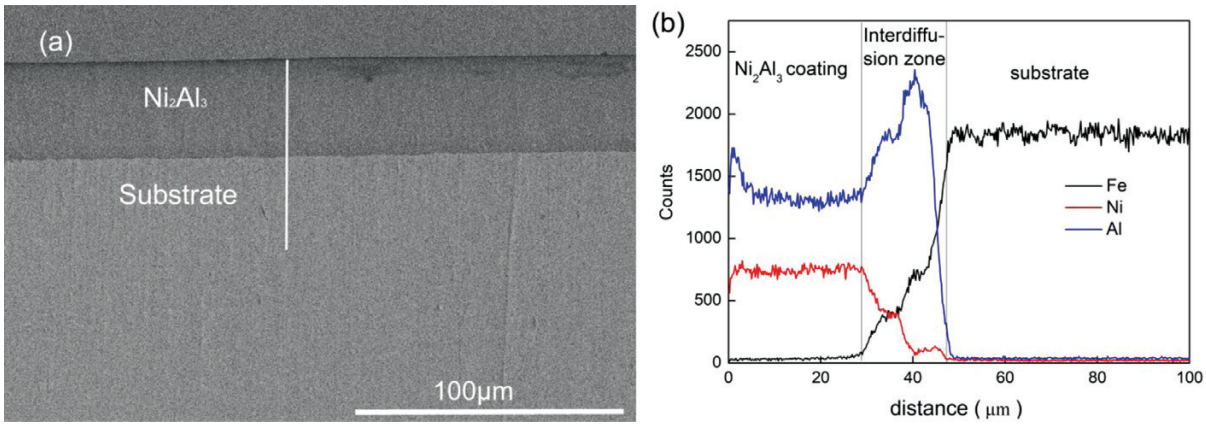

Figure 3: Cross-sectional microstructure and composition of the Ni_2Al_3 coating

coating, fabricated with an 8 *w*/% pack Al-powder amount. It can be seen from **Figure 3a** that the aluminized layer is composed of the surface Ni_2Al_3 coating and an interdiffusion zone in the center. The Ni_2Al_3 layer and substrate are clearly distinguished in **Figure 3a**, while the interdiffusion layer is not easily observed on the backscatter image. **Figure 3b** shows that the Ni_2Al_3 coating thickness is approximately 30 μm with a low Fe-element content. The Ni/Al content ratio is constant throughout the coating thickness. This proves that the Ni_2Al_3 coating is a single and stable phase, which is consistent with XRD. In addition, the coating cross-section is very smooth, with no cracks at the interface, indicating a tight bond with the substrate. It can also be seen that the interdiffusion zone thickness is 20 μm, with three elements including Al, Ni and Fe. The content of Ni and Al decreases slowly, gradually penetrating the substrate. At the same time, a small amount of iron is found to be diffusing from the Q235 substrate. In addition to being different from the Ni_2Al_3 coating, the diffusion layer is also different from the substrate, which is the result of the interdiffusion between the coating and substrate, therefore leading to the metallurgical bonding with the substrate, and further enhancing the interfacial adhesion. A reduction in delamination and spalling is a unique advantage of a functionally graded layer. The reason for this is that it reduces the stress concentration and decreases the crack-driving force.

Another phenomenon that can be seen on **Figure 3b** is the fact that the Al atoms fluctuate at the beginning and then reach a relative stability. A possible reason for this is the fact that the sample surface is in direct contact with the pack cement agent during the aluminizing process, enhancing the activity of the Al atoms, while after aluminizing, rich Al atoms are not evenly spread, thus resulting in a high Al content on the surface. Later the Al atoms are stabilized throughout the coating thickness.

3.4 Hardness of the functionally graded Ni_2Al_3 coating

Nanoindentation is also known as a depth-of-indentation sensitive method, which has been used for precision measuring of hardness, elastic modulus and other mechanical properties of various materials in recent years.[14,15] It can directly determine a contact area in real time through a load-displacement curve, instead of measuring the surface indentation with an optical method, thus significantly reducing errors.[16] Its theory is based on the Oliver-Pharr method for calculating the hardness and elastic modulus. In addition to considering the unloading curve, this method also considers the indenter shape and the indentation depth to calculate the contact area under a load.

Figure 4 shows a typical load-displacement curve of the nanoindentation test. The symbols represent the following: P_{max} is the maximum load, h_{max} is the deepest penetration depth, S is the contact stiffness (the initial slope of the unloading curve), and h_f is the residual displacement after complete unloading. The measurement process is divided into three stages: loading, load holding and unloading. Through the testing and analysis, the hardness (H) and elastic modulus (E) values for different materials can be obtained, to find out whether the coating can improve the substrate property.

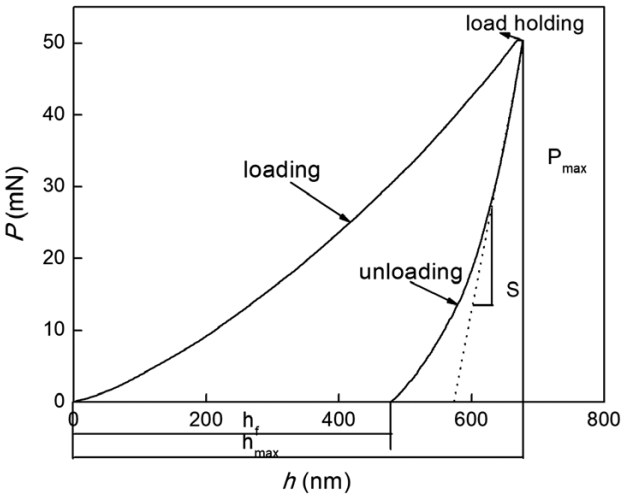

Figure 4: Typical load-penetration depth curves obtained with a nanoindentation test

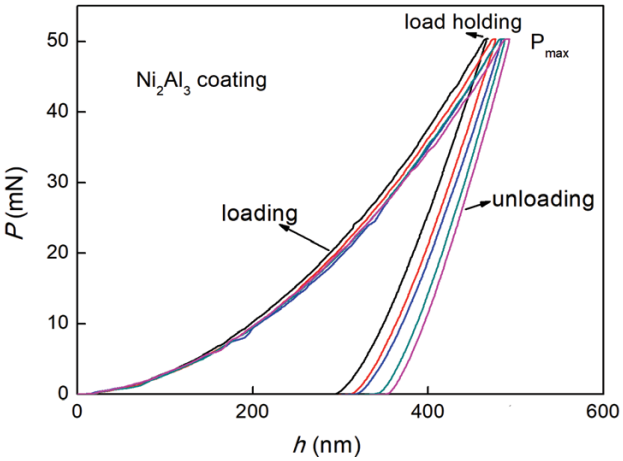

Figure 5: Load-penetration depth curves for the Ni_2Al_3 coating

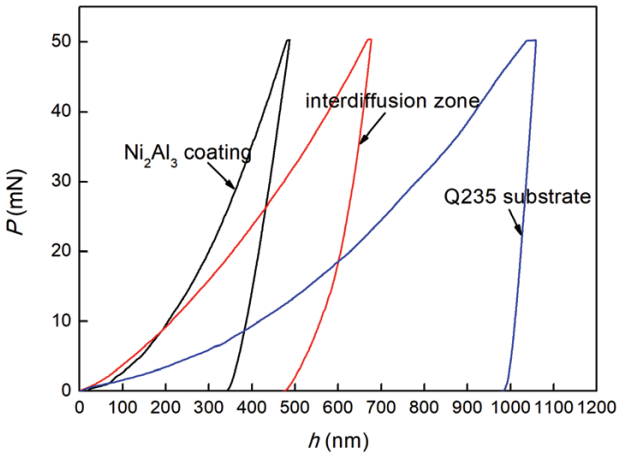

Figure 6: Load-depth curves obtained with the nanoindentation test of different coating regions

Load-penetration depth curves for the Ni_2Al_3 coating are shown in **Figure 5**. As can be seen, five turns are on the same trend, though exhibiting low discrete variables. **Table 4** reveals specific data, verifying the change in the hardness. Finally, the average hardness H of the Ni_2Al_3 coating is about 15.05 GPa, and the elastic modulus E is 227.59 GPa. The value of H/E is characterized by the material wear resistance to some extent.[17]

The same method is used to measure different coating regions, to verify whether the coating improves the property of the substrate, and the specific figures and data are shown in **Figure 6** and **Table 5**. For comparison, only one group of data is selected for the analysis. It is evident that the hardness value of the substrate is the lowest, while its values for h_{max}, h_f and S are the largest. In contrast, the hardness value of the surface Ni_2Al_3 coating is the highest, while h_{max}, h_f and S are the lowest. From the coating surface to the interdiffusion layer, and then to the internal substrate, the value of H/E is gently decreased, thereby a gradient change in the performance is realized. The size of the area surrounded by the curve indicates a plastic material. As can be seen, the nanoindentation area of Ni_2Al_3 is more compact than the interdiffusion zone and substrate, including smaller regions and indicating a less plastic deformation of the coating in the loading process. This is in line with the high hardness of the Ni_2Al_3 layer: the greater the hardness, the smaller is the plastic deformation under the same pressure. It can also be seen that the variety in the pressing depth of the coating is the smallest, within the same holding time.

Figure 7 represents the morphology after the nanoindentation. Although each area was detected five times, only two groups appear in this image due to a limited range of the camera, but the difference can still be

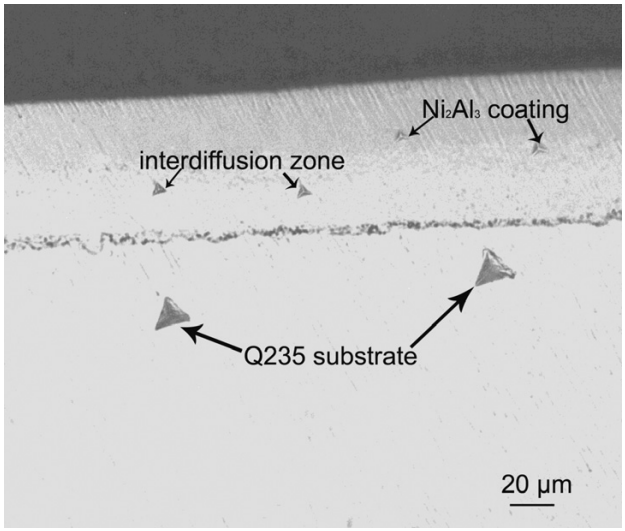

Figure 7: Morphology of different regions measured with nanoindentation

Table 4: Specific data for the Ni_2Al_3 coating measured with nanoindentation

Parameter	1	2	3	4	5	Mean
H (MPa)	16589.46	15561.99	15124.08	14169.13	13789.45	15046.82
E (GPa)	221.80	221.72	215.26	239.53	239.62	227.59

Table 5: Nanoindentation test data for varying coating regions

Material	H (MPa)	E (GPa)	h_{max} (nm)	h_f (nm)	S (mN/nm)
Q235 substrate	2543.1	203.2	1044.54	974.11	0.8994
Interdiffusion zone	6614.5	175.6	676.92	482.49	0.5317
Ni_2Al_3 coating	15046.82	227.59	481.43	329.55	0.4389

noticed. It can be concluded from **Figure 7** that under the same pressure, the indentation size and deformation of the Ni_2Al_3 coating are the smallest, and a triangular pyramid shape can be seen. However, the indentation size and deformation of the interdiffusion zone are in the middle, while the matrix is the largest. A more significant deformation indicates a lower hardness and a deeper indentation depth. Similarly, the value of the unloading-curve initial slope *S* is also larger. Therefore, it can be concluded that the hardness of the Ni_2Al_3 coating is the highest, which is also consistent with the previous test data from **Table 5**.

3.5 Formation analysis of the Ni_2Al_3 coating

The formation of the Ni_2Al_3 coating is analyzed below, as shown in the relation[18,19] where *X* stands for one element out of F, Cl or Br, *n* is an integer of less than 3, and the range of *y* is more than 1/3, but less than 3.

$$Al + AlX_3 \rightarrow AlX_n \quad (1)$$

$$AlX_n + Ni \rightarrow AlNi_y + AlX_3 \quad (2)$$

For this research, *X* indicates Cl. A brief analysis is as follows. The low aluminizing temperature promotes the inward diffusion of aluminum. The $AlCl_n$ gas phase is formed due to the contact between the Al powder and activator $AlCl_3$, which is a crucial step in the formation. $AlCl_n$ is more thermally stable than $AlCl_3$ as the temperature increases. After that, $AlCl_n$ reacts with the nickel-plated surface to deposit aluminum atoms. An intermetallic layer forms on the surface, with an AlNiy composition of ($1/3 \leq y \leq 3$). As the aluminum atoms are brought to the surface by a gaseous-state process, a solid-phase diffusion follows. The generated activator $AlCl_3$ returns to the aluminum source to continue the process. When *X* represents F or Br, a similar chemical reaction occurs.

This process is different from pack aluminizing of a nickel-base superalloy surface.[20] The general reason for it is that there are two noticeable differences in the chemical composition and precipitation phase between the nickel-plated substrate and nickel-base superalloy. The electroplated nickel layer is a single γ phase, while the nickel-base superalloy includes a γ solid solution as well as multiple precipitation phases, namely the γ and carbide phase; at the same time, solution elements Mo and Co increase the activation energy of the vacancy formation. The presence of residues reduces the effective diffusion zone, leading to an extension of the diffusion path. Therefore, high-temperature aluminizing is applied on the nickel-base superalloy, while the nickel-plated substrate can be aluminized at a low temperature to reduce the impact on its properties.

The microstructure and chemical composition of the aluminized layer exhibit a gradual change. As a result, the hardness also changes gradually, effectively reducing the stress. This is the advantage of functionally gradient materials. Instead of the traditional homogenous material coatings, FGM coatings do not only improve the connection strength and reduce the crack-driving force, but they also endue excellent friction and wear properties of materials.

4 CONCLUSIONS

From the study, the following conclusions can be drawn:

1) A single Ni_2Al_3 coating phase can be prepared with an 8 *w*/% Al content of pack cement. There is a transition zone between the coating and substrate. The thickness of the Ni_2Al_3 layer is approximately 30 μm, with a low content of the Fe element. The interdiffusion zone thickness is 20 μm, with three elements including Al, Ni and Fe.

2) The average hardness of the Ni_2Al_3 layer is about 15.05 GPa, which is higher than those of the interdiffusion zone and Q235 substrate that are 6.6 GPa and 2.5 GPa. The indentation size and deformation of the Ni_2Al_3 coating are the smallest, with a triangular pyramid shape.

Acknowledgment

This research was funded by the Key R&D and Promotion Special (Scientific Problem Tackling) Project of the Henan Province (No. 212102210039), Science and Technology Collaborative Innovation of the Zhengzhou Project in 2022 and the High-Level Introduction of Talent Research Start-Up Fund of the North China University of Water Resources and Electric Power (No. 4001/40680).

5 REFERENCES

[1] Y. Tang, Z. S. Ma, Q. Ding, T. Wang, Dynamic interaction between bi-directional functionally graded materials and magneto-electro-elastic fields: A nano-structure analysis, Compos. Struct., 264 (**2021**) 8, 113746, doi:10.1016/j.compstruct.2021.113746

[2] M. J. Yu, A. X. Feng, L. J. Yang, M. E. Thomas, Microstructure and corrosion behaviour of 316L-IN625 functionally graded materials via laser metal deposition, Corros. Sci., 193 (**2021**), 109876, doi:10.1016/j.cors ci.2021.109876

[3] S. Chandrasekaran, S. Hari, M. Amirthalingam, Functionally graded materials for marine risers by additive manufacturing for high-temperature applications: Experimental investigations, Structures, 35 (**2022**), 931–938, doi:10.1 016/j.istruc.2021.12.004

[4] E. Damerchi, A. Abdollah-zadeh, R. Poursalehi, M. S. Mehr, Effects of functionally graded TiN layer and deposition temperature on the structure and surface properties of TiCN coating deposited on plasma nitrided H13 steel by PACVD method, J. Alloy. Compd., 772 (**2019**), 612–624, doi: 10.1016/j.jall com.2018.09.083

[5] T. J. Levingstone, N. Barron, M. Ardhaoui, K. Benyounis, L. Looney, J. Stokes, Application of response surface methodology in the design of functionally graded plasma sprayed hydroxyapatite coatings, Surf. Coat. Tech., 313 (**2017**), 307–318, doi:10.1016/j.surfcoat.2017.01.113

[6] R. R. Behera, A. Hasan, M. R. Sankar, L. M. Pandey, Laser cladding with HA and functionally graded TiO_2-HA precursors on Ti–6Al–4V

alloy for enhancing bioactivity and cyto-compatibility, Surf. Coat. Tech., 352 (**2018**), doi: 10.1016/j.surfcoat.2018.08.044

[7] X. Z. Fan, L. Zhu, W. Z. Huang, Investigation of NiAl intermetallic compound as bond coat for thermal barrier coatings on Mg alloy, J. Alloy. Compd., 729 (**2017**), 617–626, doi:10.1016/j.jallcom.2017.09.190

[8] X. Chen, C. Li, S. J. Xu, Y. Hu, G. C. Ji, H. T. Wang, Microstructure and Microhardness of Ni/Al-TiB2 composite coatings prepared by cold spraying combined with postannealing treatment, Coatings., 9 (**2019**) 9, 565, doi:10.3390 /coatings9090565

[9] X. X. Zhao, X. M. Li, M. F. Li, C. G. Zhou, Comparison of the corrosion resistance of Ni_2Al_3 coating with and without Ni-Re interlayer in dry and wet CO_2 gas, Corros. Sci., 159 (**2019**), 108121, doi:10.1016/j.corsci. 2019. 108121

[10] Y. D. Wang, Y. P. Zhang, G. Liang, Q. L.Ding, Low temperature formation of aluminide coatings on the electrodeposited nanocrystalline Ni and its oxidation resistance with La_2O_3/CeO_2 nanoparticle dispersion, Vacuum, 173 (**2020**), 109148, doi:10.1016/j.vacuum.2019.109148

[11] Y. T. Zhao, Z. H. Tian, B. B. Li, H. P. Ren, Effect of rare earth (CeCl3) on oxidation resistance of Ni_2Al_3/Ni composite coatings on heat-resistant steel, Rare. Metal. Mat. Eng., 48 (**2019**) 11, 3452–3432, doi:CNKI: SUN: COS E.0.2019-11-002

[12] X. M. Yuan, H. G. Yang, W. W. Zhao, Q. Zhan, X. X. Zhu, Study on pack cementation process for preparation of low activity pack aluminizing layer on RAFM steel, Mat. Rev., 29 (**2015**), 66–68, doi:10.1530/acta.0.0570 557

[13] A. Thevand, S. Poize, J. P. Crousier, R. Streiff, Aluminization of nickel-formation of intermetallic phases and Ni_2Al_3 coatings, J. Mater. Sci., 16 (**1981**), 2467–2479, doi:10.1007/BF01113583

[14] L. Chitsaz-Khoyi, J. Khalil-Allafi, A. Motallebzadeh, M. Etminanfar, The effect of hydroxyapatite nanoparticles on electrochemical and mechanical performance of TiC/N coating fabricated by plasma electrolytic saturation method, Surf. Coat. Tech., 394 (**2020**), 125817, doi:10.1016/j.surfcoat.2020.125817

[15] H. H. Ding, V. Fridrici, G. Guillonneau, S. Sao-Joao, J. Fontaine, P. Kapsa, Investigation on mechanical properties of tribofilm formed on Ti–6Al–4V surface sliding against a DLC coating by nano-indentation and micro-pillar compression techniques, Wear, 432–433 (**2019**), 202954, doi:10.1016/j.wear.2019.202954

[16] H. Y. Lee, J. H. Lee, Evaluation of material characteristics by micro/nano indentation tests, T. Kor. Soc. Mec. Eng. A., 32 (**2008**) 10, 805–816, doi:10.3795/KSME-A.2008.32.10.805

[17] R. Yang, T. H. Zhang, P. Jiang, Y. L. Bai, Experimental verification and theoretical analysis of the relationships between hardness, elastic modulus, and the work of indentation, Appl. Phys. Lett., 92 (**2008**) 23, 1906, doi:10.1063/1.2944138

[18] X. Xiang, F. L Yang, G. K. Zhang, X. L. Wang, Effect of steel substrates on the formation and deuterium permeation resistance of aluminide coatings, Coatings, 9 (**2019**) 2, 95, doi:10.3390/coatings9020095

[19] F. Shahriari, F. Ashrafizadeh, A. Saatchi, Formation and characterisation of NiAl-Ti coating on nickel-based superalloy B1900, Surf. Interface Anal., 41 (**2009**) 5, 378–383, doi:10.1002/sia.3031

[20] H. Rafiee, S. Rastegari, H. Arabi, M. Mojaddam, Effects of temperature and Al-concentration on formation mechanism of an aluminide coating applied on superalloy IN738LC through a single step low activity gas diffusion process, J. Alloy. Compd., 7 (**2010**) 4, 42–49, doi:10.1016/j.jallcom.2010.06.030